

# Combined Command Shaping and Inertial Damping for Flexure Control

David P. Magee  
Texas Instruments, Inc.  
P.O. Box 655474, MS 446  
Dallas, TX 75265  
magee@ti.com

David W. Cannon  
Georgia Institute of Technology  
Mechanical Engineering Dept.  
Atlanta, GA 30332-0405  
dcannon@mindspring.com

Wayne J. Book  
Georgia Institute of Technology  
Mechanical Engineering Dept.  
Atlanta, GA 30332-0405  
wayne.book@me.gatech.edu

## Abstract

*This paper describes a new control approach that combines command shaping and inertial damping to control small robots that are attached to the end of a flexible manipulator. The command shaping guarantees that the level of vibration will be minimized during the robot motion and the inertial damping removes any residual effects after the motion is complete. Experimental results from two different test beds verify the effectiveness of the combined approach for minimizing vibration in elastic systems.*

## 1. Introduction

Singer and Seering [1] developed an input shaping method based on delayed inputs that could be used to exactly cancel the vibratory motion of linear flexible systems given knowledge of only the natural frequency and damping ratio of each mode. They also showed how robustness could be achieved by including additional filter terms. Singh and Vadali [2] showed that the robustness corresponds to multiple zeros placed to cancel the vibratory poles. Rappole, Singer and Seering [3] generalized the original Singer and Seering result and Magee and Book [4] showed how to place multiple zeros at the desired location with an arbitrarily small time-delay value. The small time-delay is desirable to complete the response as quickly as possible and to ensure stability when the filter is placed inside a feedback loop. The shortened time-delay results in magnitudes of the frequency response greater than one for some high frequencies, compromising this advantage, however. The compromise is a combination of concern for stability and for increased excitation of the higher flexible modes.

Inertial damping has been illustrated to be effective by several authors [5-7]. Lee [5] implemented a robust control on the GT (Georgia Tech) test bed. Lew [6] illustrated a dramatically effective and yet simple implementation on the PNNL (Pacific Northwest National Laboratory) test bed based on strain measurements at the base of the flexible link. Lew's implementation is most effective when a small arm is in a configuration that strongly couples the inertial forces generated by the small arm to the appropriate modes of vibration of the large arm. Sharf [7] simulated a damping algorithm that could generate appropriate inertial forces regardless of the small arm's

configuration. However, for this approach, the damping function was not integrated with the task functioning of the small arm. Also, no experimental results were presented with the more computationally complex Sharf algorithm.

## 2. Control Approach

In this paper, inertial damping will be combined with a more general command shaping algorithm to produce an effective macro-micro manipulator vibration controller. Figure 1 shows a general block diagram of this approach.

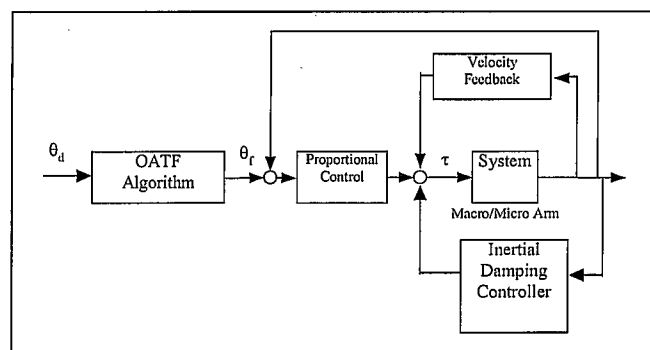


Figure 1 Combined Controller Implementation

The command shaping is guaranteed to minimize the level of vibration during the micro-manipulator's motion and the inertial damping removes any residual vibration effects after the motion is complete. The next two subsections are a brief overview of each technique but the reader should consult [8, 9] for more detailed discussions.

### 2.1 OATF Algorithm

Over the last eight years, there have been many improvements to the original input shaping algorithm by Singer and Seering [1]. Recently, Magee developed a very general filtering algorithm for any number of elastic modes of vibration, called an OATF (Optimal Arbitrary Time-delay Filter) Algorithm [9], that minimizes the cost function

$$J(t) = \frac{1}{2} e^T(t) W_1 e(t) + \frac{1}{2} \dot{e}^T(t) W_2 \dot{e}(t) \quad (1)$$

where  $e(t)$  is the error in the desired elastic generalized coordinates and  $W_i$  are weighting matrices between errors in position and velocity, respectively. The filter solution to the

optimization problem for one mode of vibration can be written as

$$f(t) = \delta(t) - 2\cos(\omega_d T_1) e^{-\zeta \omega_n T_1} \delta(t - T_1) + e^{-2\zeta \omega_n T_1} \delta(t - 2T_1) \quad (2)$$

for any finite and nonzero time-delay value  $T_1$ . This filter was initially discovered by Magee and Book as pole-zero cancellation of unwanted oscillatory dynamics that occurred independently of the time-delay value [4].

The latest research results demonstrate the robustness characteristics of the new filtering algorithm with respect to system parameter uncertainty. Figure 2 shows a three-dimensional plot of the vibration error due to uncertainty in the natural frequency of the system. Any region where the vibration error is below a pre-defined level is considered a location where robustness exists in the filtering algorithm. In this example, the filter is said to be robust for any vibration error less than 5%. However, this vibration error level can change depending on the application.

The variables  $T_1^*$  and  $T_a^*$  in the figure represent normalized periods of time (time-delay value and period of oscillation) with respect to the modeled period of system oscillation,  $T_n$ . By normalizing the graph in this manner, the results can be easily applied to any system.

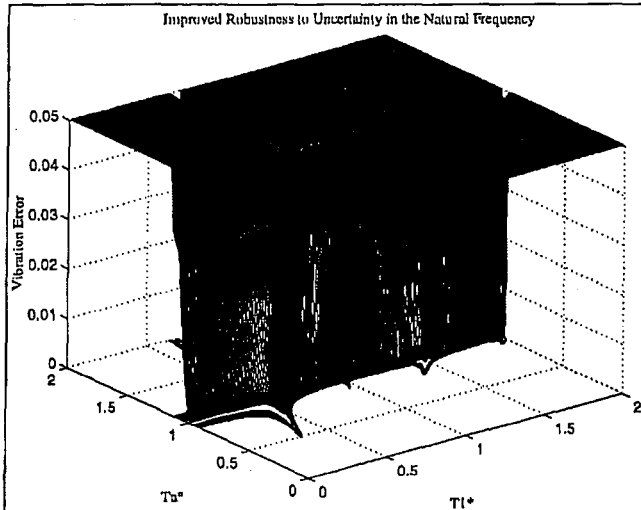


Figure 2 Robustness to Uncertainty in Natural Frequency

This particular robustness plot corresponds to an OATF algorithm that places two sets of zeros near the oscillatory pole location for any nonzero and finite time-delay value. For this filter, several regions of robustness can be found in Figure 2. For example, a robustness trench exists along the line where  $T_1^* \approx 1$ . This result makes sense because in the ideal modeling scenario,  $T_n = T_a$ . A second region of robustness occurs near the point  $T_1^* \approx 0.5$  and  $T_a^* \approx 1$ . This region is where this particular OATF algorithm places four

sets of zeros at the oscillatory pole location. In fact, this particular time-delay value corresponds to the input shaping algorithm of Singer and Seering. Later experimental results will also suggest that this region provides the best improvement for reducing the level of vibration when compared to PD control alone.

## 2.2 Inertial Damping

Cannon, Magee, Book and Lew initially experimented with an inertial damping controller in [10]. By feeding back beam strain to a joint controller, settling times could be reduced by over 97%. This reduction was offset by an increase in joint settling time. Cannon [8] then showed that beam tip acceleration could be used as the feedback in the inertial damping controller with similar results.

To investigate this feedback effect on the system, the poles of a linearized system are investigated as the feedback gain is increased. The dynamics for a one degree-of-freedom micro-manipulator attached to the end of a flexible beam can be written as

$$\begin{bmatrix} \left( \frac{33}{140} M_b + M + m - \frac{3K_a}{2L} \right) & -ml \\ -ml - K_a & ml^2 + I_x \end{bmatrix} \begin{bmatrix} \ddot{q}_1 \\ \ddot{q}_2 \end{bmatrix} + \begin{bmatrix} \frac{d}{2L} & 0 \\ \frac{3K_v}{2L} & K_v \end{bmatrix} \begin{bmatrix} \dot{q}_1 \\ \dot{q}_2 \end{bmatrix} + \begin{bmatrix} \frac{3EI}{L^3} & \frac{3K_p}{2L} \\ 0 & K_p \end{bmatrix} \begin{bmatrix} q_1 \\ q_2 \end{bmatrix} = \begin{bmatrix} \frac{3K_p}{2L} \\ \frac{3K_p}{K_p} \end{bmatrix} \theta_d \quad (3)$$

where

- $M_b$  is the mass of the beam
- $M$  is the mass of the micro-manipulator base
- $m$  is the mass of the micro-manipulator link
- $L$  is the length of the beam
- $l$  is the distance to the cg of the link
- $E$  is the Young's modulus for the beam
- $I$  is the area moment of inertia for the beam
- $\bar{q}_i$  is the  $i^{th}$  linearized generalized coordinate
- $\theta_d$  is the desired joint angle position

The equation is derived using the dominant mode in an assumed modes model. The rigid manipulator joint controller consists of a PD, proportional with velocity feedback, controller combined with beam tip acceleration feedback.  $K_p$  and  $K_v$  are the PD joint-controller gains while  $K_a$  is the inertial damping feedback gain. A full derivation can be found in [10].

As Equation (3) shows, the acceleration feedback gain  $K_a$  affects the mass matrix by lowering the effective mass of the beam and increasing the effect of the beam tip acceleration on the micro arm dynamics. Figure 3 shows a pole map of the system as the gain  $K_a$  is increased. The dominant closed loop poles of the system representing beam tip motion move away from the  $j\omega$  axis and toward the real

pole map of the system as the gain  $K_a$  is increased. The dominant closed loop poles of the system representing beam tip motion move away from the  $j\omega$  axis and toward the real axis as the gain increases. At the same time, the damping ratios of the system increase while the natural frequencies of the system decrease slightly.

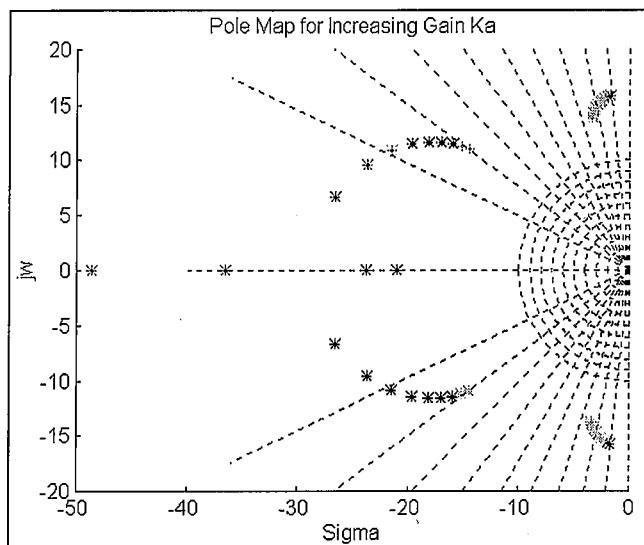


Figure 3 Pole Map

### 3. Manipulator Test Beds

Experimental results from two different test beds will be presented in this paper. The PNNL test bed was used to verify the concept of the combined controller and the GT test bed was used to investigate the proposed controller in a more structured and well known environment.

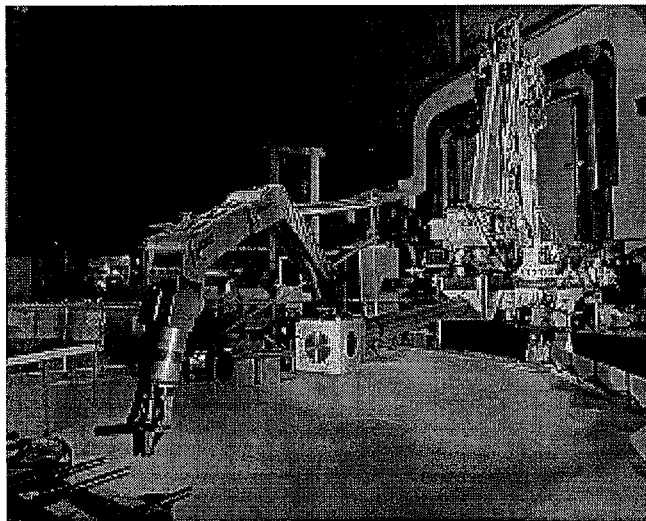


Figure 4 PNNL Test Bed

#### 3.1 PNNL Test Bed

The PNNL test bed consists of a flexible beam attached to a SPAR 2500 heavy lift manipulator which carries a Schilling Titan II, shown in Figure 4. The 3.4 m aluminum beam gives the manipulator a 12 m reach. The design has a reach and fundamental natural frequency similar to the micro-macro manipulator system proposed for use in large nuclear waste underground storage tanks [11].

The beam's natural frequencies and damping ratios were calculated from experimental data taken from an impulse response. The lowest natural frequency is 2.14 Hz in the vertical plane with a damping ratio of 0.006. The second natural frequency is near 10.5 Hz, but is very small in amplitude. In the horizontal direction, the natural frequencies are the same, but the damping ratios are near 0.03. Strain gauges located at the base of the beam provide the beam's flexural displacement.

The Schilling Titan II is oriented on the end of the beam so that the first axis of rotation is always perpendicular to the horizontal plane and the second axis is always perpendicular to vertical direction. This orientation decouples the inertial forces generated by movements in these two planes.

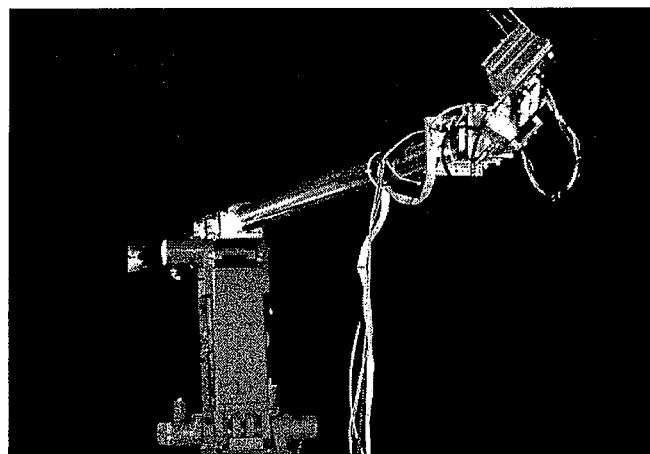


Figure 5 GT Test Bed

#### 3.2 Georgia Tech Test Bed

The GT test bed consists of one flexible link and three rigid degrees of freedom [8]. The flexible link is comprised of a 10 ft. aluminum beam. The beam is attached to an existing Cincinnati Milacron T3-646, as shown in Figure 5, which is assumed to be a rigid base.

The rigid micro-manipulator consists of three direct drive links. The experimental results are based on a one degree-of-freedom micro manipulator so the first and third links were immobilized. The effective center of mass becomes 0.244 m, the mass becomes 7.076 kg, and the

moment of inertia becomes  $0.08172 \text{ kg-m}^2$ . The resulting natural frequency and damping ratio were experimentally determined to be  $3.064 \text{ Hz}$  and  $0.014$ , respectively.

#### 4. Experimental Results

The PNNL test bed provided initial verification that a combined command shaping and inertial damping controller can be combined with an ordinary PD controller. Figure 6 compares the Schilling's response for a  $15^\circ$  slew of the first joint. Although the joint angle response time is increased by more than one second, the general shape of the trajectory remained the same.

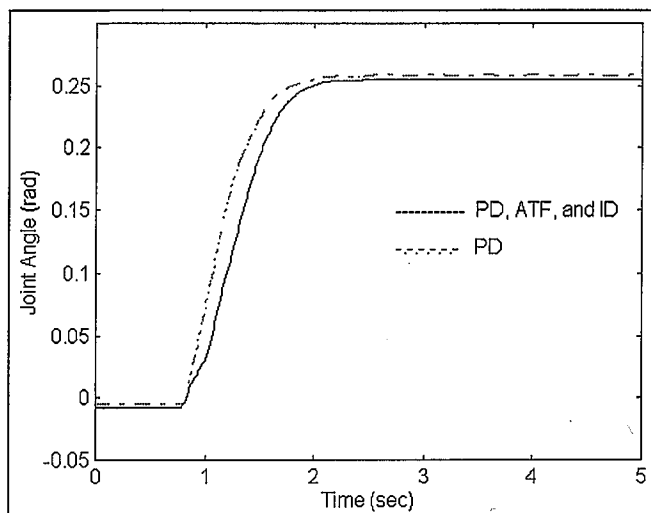


Figure 6 PNNL Joint Response Comparison

The vibration reduction for the  $15^\circ$  slew of the first joint can be verified in the beam strain measurement shown in

Figure 7. The settling time for the oscillation is reduced from over 40 seconds for the PD controller alone to under 4 seconds for the combined controller.

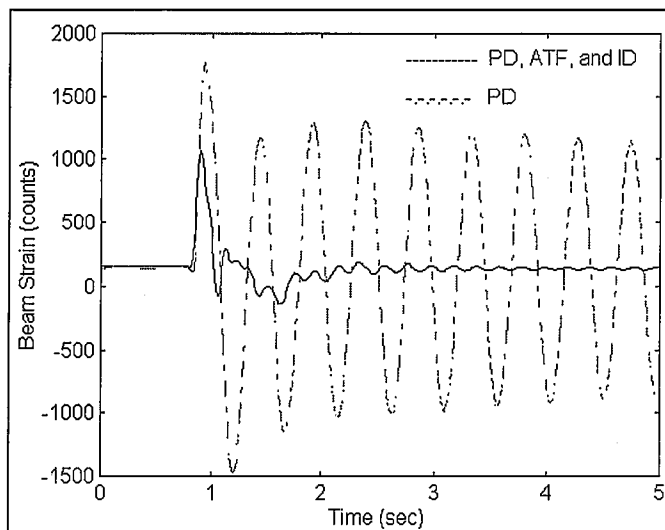


Figure 7 PNNL Beam Response Comparison

The focus of the experimental investigation will now shift to the GT test bed where the micro-manipulator is commanded to follow a  $15^\circ$  slew of the second joint. Figure 8 compares the joint responses for PD control alone and with the command shaping and inertial damping, called the Manipulator Vibration Controller (MVC). Once again, the only noticeable difference is the time delay introduced by the OATF algorithm which amounts to  $0.3$  seconds.

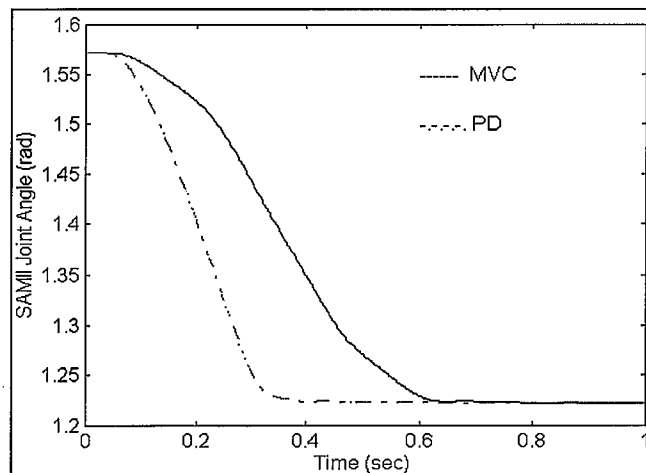


Figure 8 GT Joint Response Comparison

The significant difference in the experimental results from the GT test bed appears when comparing the level and duration of vibration during the  $15^\circ$  slew. Figure 9 shows the vertical acceleration at the tip of the beam for the slew motion. The maximum level of vibration is reduced by 80% and the oscillation duration is reduced from over 15 seconds to less than one second.

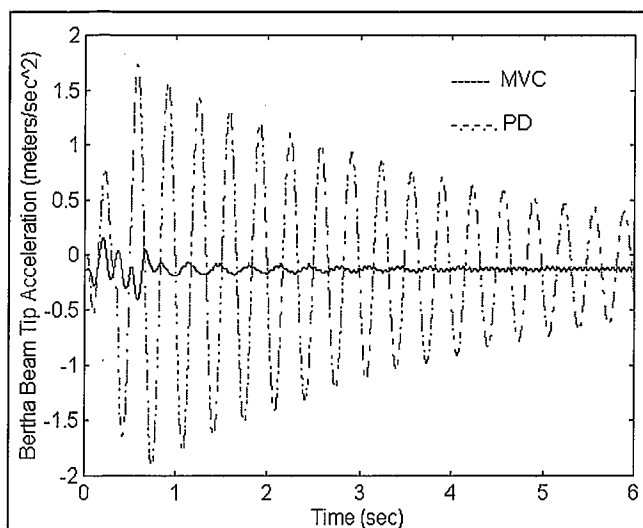


Figure 9 GT Beam Response Comparison

The experimental results from the two macro-micro manipulator test beds have definitely demonstrated the vibration suppression ability of the combined control approach but the effect of the arbitrary time-delay value on the results has not been discussed. Several experiments were therefore conducted on the GT test bed to determine if definite trends exist. Figure 10 shows the amount of improvement in maximum acceleration response that is provided by the OATF algorithm in the combined controller over just PD alone. This figure suggests that there is indeed a range of ideal time-delay values that maximizes the improvement. In fact, this range corresponds to the large robustness region in Figure 2 near the point  $T_1^* \approx 0.5$  and  $T_a^* \approx 1$ .

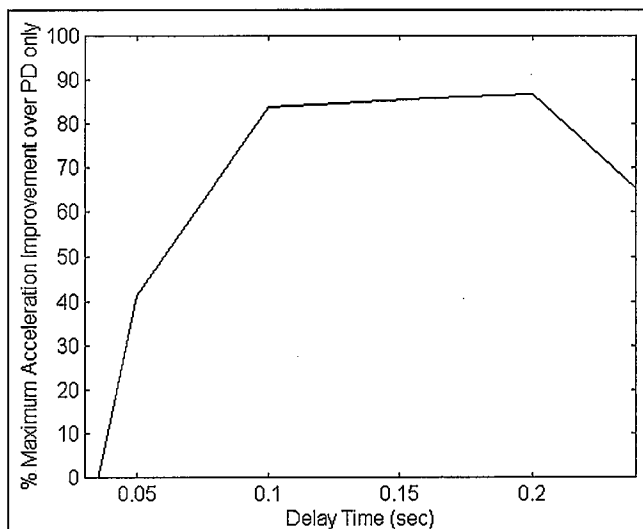


Figure 10 Maximum Tip Acceleration Trends

## 5. Conclusions

This paper investigated a combined control approach for minimizing the level of vibration during commanded motions of a macro-micro manipulator system. By shaping the desired trajectory during the motion, the level of vibration is guaranteed to be minimized by the OATF algorithm. To account for any model uncertainty or external disturbances, inertial damping was also incorporated into the control strategy. The overall stability of the command shaping and inertial damping controller for a linearized system was then analyzed to support the combined approach.

This flexure control system was then experimentally verified on two separate test beds to demonstrate its effectiveness as a macro-micro manipulator vibration controller. The time-delay trends from the experiments were then related back to theoretical performance measures to further justify the effectiveness of the combined command shaping and inertial damping controller.

## 6. Acknowledgments

This research was partially supported through Sandia National Laboratories, Contract No. AK-9037.

## 7. References

1. Singer, N.C. and W.P. Seering, "Preshaping Command Inputs to Reduce System Vibration," *ASME Journal of Dynamic Systems, Measurement, and Control*, Vol.112, No.1, 1990, pp.76-82.
2. Singh, T. and S.R. Vadali, "Robust Time-Delay Control," *ASME Journal of Dynamic Systems, Measurement, and Control*, Vol.115, No.2A, 1993, pp.303-306.
3. Rappole, B.W., Jr., N.C. Singer, and W.P. Seering, "Input Shaping with Negative Sequences for Reducing Vibrations in Flexible Structures", *Proceedings of the American Control Conference*, Vol.3, San Francisco, CA, June 2-4, 1993, pp.2695-2699.
4. Magee, D.P. and W.J. Book, "Filtering Micro-Manipulator Wrist Commands to Prevent Flexible Base Motion", *Proceedings of the American Control Conference*, Vol.1, Seattle, WA, June 21-23, 1995, pp.924-928.
5. Lee, S.H. and W.J. Book, *Robot Vibration Control Using Inertial Damping Forces*, in *8th CISM-IFTOMM Symposium on the Theory and Practice of Robots and Manipulators*. 1990: Cracow, Poland.
6. Lew, J.Y., et al. "Micro Manipulator Control to Suppress Macro Manipulator Structural Vibrations", *Proceedings of the IEEE International Conference on Robotics and Automation*, Vol.3, Nagoya, Aichi, Japan, May 21-27, 1995, pp.3116-3120.

7. Sharf, I. "Active Damping of a Large Flexible Manipulator with a Short-Reach Robot", *Proceedings of the American Control Conference*, Vol.5, Seattle, WA, June 21-23, 1995, pp.3329-3333.
8. Cannon, D.W., *Command Generation and Inertial Damping Control of Flexible Macro-Micro Manipulators*, MS Thesis, Georgia Institute of Technology, 1996.
9. Magee, D.P., *Optimal Arbitrary Time-delay Filtering to Minimize Vibration in Elastic Manipulator Systems*, Ph.D. Thesis, Georgia Institute of Technology, August 1996.
10. Cannon, D.W., *et al.* "Experimental Study on Micro/Macro Manipulator Vibration Control", *Proceedings of the IEEE International Conference on Robotics and Automation*, Vol.3, Minneapolis, MN, April 22-28, 1996, pp.2549-2554.
11. Kwon, D.S., *et al.* "Parametric Design Studies of Long-Reach Manipulators", *Proceedings of the ANS Fifth Topical Meeting on Robotics and Remote Systems*, Vol.1, Knoxville, TN, April 25-28, 1993, pp.265-273.